SUPPORTING INFORMATION:

The nanoporous gold (np-Au) film was characterized optically with a Sentech SE-850 spectroscopic ellipsometer. Transmission and reflection spectra were used to calculate the absorbance spectrum, and spectroscopic ellipsometry confirmed that the film's thickness was 150 nm. These measurements were used to derive the extinction cross section spectrum in Figure 1 (red line), assuming, based on SEM data, that the average np-Au particle in the 50% Au/50% air film is a sphere of radius 10 nm. A 150-nm thick film of continuous Au deposited on SiO_2 by evaporation was also studied with the Sentech SE-850, and its transmission and reflection spectra were used to determine its absorbance spectrum. The np-Au film has a broad extinction spectrum that shows a peak between 300 and 400 nm, and a tail that decreases with increasing wavelength through most of the visible. Though the absorbance cross sections of both np- and bulk Au peak at similar wavelengths, the percent absorbance of np-Au is more than 2.5 times that of planar bulk Au throughout the visible, and np-Au absorbs over a broader wavelength range than bulk Au. Indeed, we found for nc-Si in SiO_2 coupled to a planar, continuous film of bulk Au that the luminescence intensity was decreased at all separation distances, relative to a reference sample.[1] According to Mie-Gans theory[2], the measured np-Au extinction cross section in Figure 1 is consistent with the aggregate surface plasmon resonant response for a continuum of features including Au spheres and spheroids in air and spherical and spheroidal voids in gold.

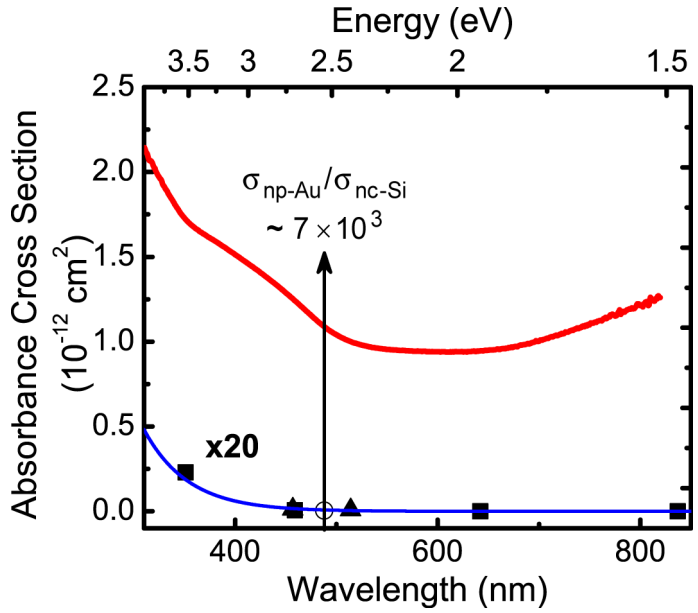

Supporting Information Figure 1. Red line: extinction cross section of np-Au as a function of absorbance wavelength. Blue line: fit to nc-Si absorbance cross section as measured at 780 nm in reference 3 (solid triangles), reference 4 (solid squares), and the present work (open circle). At the pump wavelength, λ_{ex} = 488 nm, used in this experiment, the nanoporous gold film has an extinction cross section that is 7000 times greater than that of nc-Si.

At the range of excitation wavelengths in Figure 1, the extinction cross section of np-Au is much higher than the silicon nanocrystal (nc-Si) absorbance cross section measured at an emission wavelength of 780 nm by Garcia *et al.*[3] (solid triangles), Kovalev *et al.*[4] (solid squares), and the present work (open circle). The trend in nc-Si absorbance cross section is fit to a decreasing exponential (dotted line), and it is found that the decreasing nc-Si cross sections obey a similar trend to the np-Au cross sections, but that np-Au has a larger absorbance cross section than nc-Si at all wavelengths investigated. At the pump wavelength used in this experiment, λ_{ex} = 488 nm, the cross section of the np-Au film is more than three orders of magnitude greater than that of silicon nanocrystals. The np-Au can therefore act as a sensitizer for nc-Si, thereby increasing its effective absorbance cross section,[5] whether excited directly by a photon or indirectly by a surface plasmon. Moreover, the local field near the metal is inversely proportional to its radius, so the small ellipsoids in the np-Au will concentrate the electric field much more strongly than a planar Au film. Finally, the roughness on the surface of the np-Au contains a wide array of spatial frequencies allowing plasmons at the np-Au/SiO_2 interface to be coupled out into the radiation field, in

contrast to a planar Au film that supports a bound surface plasmon mode that propagates without radiation until it is fully absorbed.

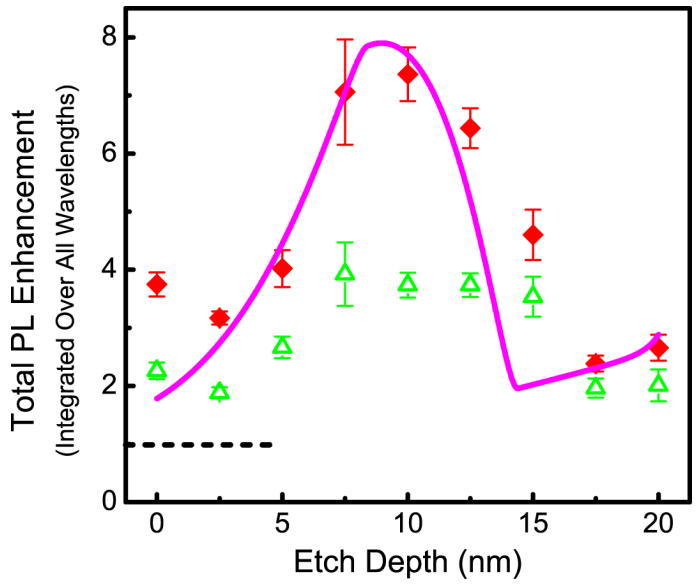

Supporting Information Figure 2. The enhancement in PL, integrated over all emission wavelengths, was measured as a function of etch depth at P_{ex} = 50 mW/mm^2 (open triangles) and 400 mW/mm^2 (closed diamonds). The solid line is a fit of the P_{ex} = 400 mW/mm^2 data to a theory that takes into account size-dependent resonant and non-resonant effects.

In Figure 2, we report the integrated intensity enhancement as a function of D. The open triangles show the PL enhancement at a low pump power, P_{ex} = 50 mW/mm^2. We find that I_{PLnpg} is greater than I_{PLref} for all D, and there is a maximum PL enhancement of ~4 when 7.5 nm < D < 15 nm. However, I_{PLref} and I_{PLnpg} varied with pump power. The dependence of I_{PLref} and I_{PLnpg} on pump power, P_{ex}, at D = 10 nm, displayed in Figure 3, shows that I_{PLref} (solid squares) increases linearly with P_{ex} up to ~120 mW/mm^2, and then grows sublinearly with further increases in P_{ex}, finally hitting its saturated intensity at P_{ex} ~ 250 mW/mm^2. The open circles in the inset of Fig. 3 show that I_{PLnpg} increases linearly with P_{ex} to ~170 mW/mm^2, and does not fully saturate for any value of P_{ex}, up to the highest experimentally attainable pump power of 417 mW/mm^2. These trends were observed for all values of D, and were most pronounced when D was between 7.5 and 12.5 nm. Due to the reduced saturation effects in the coupled np-Au/nc-Si sample, η_{PL} is more pronounced at higher pump powers: η_{PL} at P_{ex} = 400 mW/mm^2 is plotted in the filled diamonds in Figure 3; at this pump power, η_{PL} is larger than it was at the lower power, and peaks at ~7.5 when D = 7.5 – 10 nm.

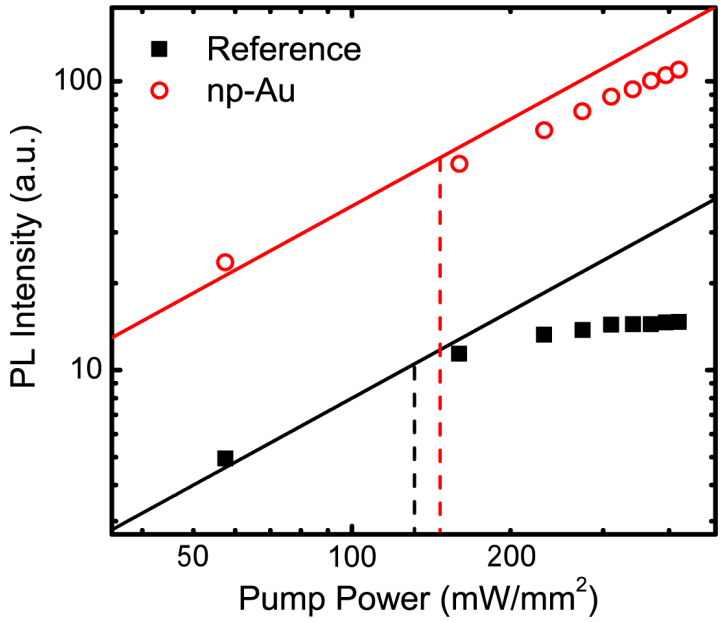

Supporting Information Figure 3. Total PL intensity integrated over all wavelengths, as a function of pump power, P_{ex}, at etch depth, D = 10 nm, for the reference sample (closed squares) and coupled sample (open circles), and fit of first data points to a linear trend from which the reference sample deviates to a greater degree than the coupled sample as a result of saturation effects. The points at which saturation begins in the reference and coupled samples are indicated by the dashed black and red lines, respectively.

At a fixed pump power, the reference sample's PL intensity and spectrum were measured as a function of etch depth, D, in the range 0 – 20 nm, and this information was used to determine the distribution of sizes and concentrations of optically active nc-Si in the sample. The sizes of the nc-Si produced from the Gaussian ion implantation profile, were inferred from the variation of average PL emission wavelength with D, due to their size-dependent exciton emission energies, and found to be depth-dependent. The measured trends indicated that smaller nanocrystals formed in the wings of the implanted excess Si^+ distribution, consistent with previous observations by Brongersma *et al.*[6] The reference sample PL intensity, I_{PLref}, was measured for each D, and the luminescence intensities were found to be consistent with a Gaussian nc-Si distribution centered at 19.2 ± 0.1 nm from the unetched surface. The separation distance between the quartz surface and the peak of the Si nanocrystal distribution at each step is therefore equal to (19.2 nm – D). The nanocrystal distribution has a width of 14.0 ± 0.6 nm. This large variance indicates that optical phenomena reported here contain contributions from nc-Si strongly coupled to np-Au as well as from non-interacting nc-Si far from the np-Au, and the quantitative analysis considers such distribution effects.

Sensitized absorption and enhanced emission are expected to be nanocrystal size dependent. As seen in Figure 1, the np-Au absorbance (red line) overlaps best with the nc-Si emission (centered at ~780 nm) between 600 and 750 nm. The smallest nanocrystals, which are found in the wings of the Gaussian nc-Si concentration profile, emit in this wavelength range, and should therefore experience resonantly enhanced emission while the larger nanocrystals experience nonresonant enhancement. We typically found in our samples that the coupled np-Au/nc-Si sample PL intensity is enhanced relative to the reference PL spectrum, the peak of the spectrum is slightly blue-shifted, and the full width at half max is slightly broadened from 125 nm to 156 nm. This is consistent with the smallest nanocrystals experiencing greater emission enhancement than larger nanocrystals.

For the total PL intensity enhancements in Figure 2, emission is resonantly enhanced in the smallest nanocrystals non-resonantly enhanced in larger nanocrystals. Though non-resonant enhancement is possible, resonant effects are predicted to be stronger.[5] At small *D*, the nanocrystals nearest the np-Au are small and are therefore resonantly enhanced, whereas for large *D*, nanocrystal emission does not occur at the plasmon resonance, even though the concentration of nanocrystals near the np-Au is large. Our model accounts for both resonant and non-resonant effects, yielding the solid line fit in Figure 2 for P_{ex} = 400 mW/mm^2.

The overall luminescence intensity enhancements, at 780 nm and integrated over the entire spectrum, are consistent with the observed enhancements in σ and Γ_{rad}, as well as Γ_{exp}. Indeed, we found that $\Gamma_{exp\text{-}npg}/\Gamma_{exp\text{-}ref} > 1$ for all the separation distances *D*, as shown in Figure 3d. In principle, the presence of np-Au can determine the increase in Γ_{exp} by enhancing both the radiative and non-radiative decay channels. Here we want to better investigate the relative importance of the two recombination paths. First of all, the radiative decay rate is enhanced by a factor 4, as shown in Figure 4 of the main text, likely because of the increased local density of states determined by the presence of the np-Au film in proximity to the

optically active Si nanocrystals. As far as the non radiative decay rate is concerned, for the reference sample we find $\Gamma_{nr\text{-}ref} = (\Gamma_{exp\text{-}ref} - \Gamma_{rad\text{-}ref)} = (45.0 - 12.4)$ kHz = 32.6 kHz. For the np-Au/nc-Si coupled sample, using the y-intercept of the straight line which best fits the data in the inset of Figure 5, i.e. $(-\Gamma_{nr\text{-}npg}/\Gamma_{rad\text{-}ref}) = -3.33$, and using the value of $\Gamma_{rad\text{-}ref}$ = 12.4 kHz, we find $\Gamma_{nr\text{-}npg}$ = 41.3 kHz. This is indeed slightly greater than the reference value, meaning that the np-Au film introduces some non-radiative paths for the Si nanocrystals; this deserves a detailed investigation.

REFERENCES:

1. Biteen, J. S.; Atwater, H. A., Unpublished Work. California Institute of Technology: 2004.

2. Bohren, C. F.; Huffman, D. R., *Absorption and Scattering of Light by Small Particles*; John Wiley & Sons, Inc.: New York, 1983.

3. Garcia, C.; Garrido, B.; Pellegrino, P.; Ferre, R.; Moreno, J. A.; Morante, J. R.; Pavesi, L.; Cazzanelli, M. *Appl. Phys. Lett.* **2003,** 82, (10), 1595-1597.

4. Kovalev, D.; Diener, J.; Heckler, H.; Polisski, G.; Kunzner, N.; Koch, F. *Phys. Rev. B* **2000,** 61, (7), 4485-4487.

5. Gersten, J.; Nitzan, A. *J. Chem. Phys.* **1981,** 75, (3), 1139-1152.

6. Brongersma, M. L.; Polman, A.; Min, K. S.; Atwater, H. A. *J. Appl. Phys.* **1999,** 86, (2), 759-763.